Heliyon

ELSEVIER

Received:
5 October 2018
Revised:
4 January 2019
Accepted:
7 March 2019

Cite as: Sinem Tunçer, Melis Çolakoğlu, Sinem Ulusan, Gülay Ertaş, Çimen Karasu, Sreeparna Banerjee. Evaluation of colloidal platinum on cytotoxicity, oxidative stress and barrier permeability across the gut epithelium. Heliyon 5 (2019) e01336. doi: 10.1016/j.heliyon.2019.e01336

Evaluation of colloidal platinum on cytotoxicity, oxidative stress and barrier permeability across the gut epithelium

Sinem Tunçer [a,1,3], **Melis Çolakoğlu** [a,2,3], **Sinem Ulusan** [b], **Gülay Ertaş** [b], **Çimen Karasu** [c], **Sreeparna Banerjee** [d,*]

[a] *Department of Biological Sciences, Orta Dogu Teknik Universitesi (ODTU/METU), Ankara 06800, Turkey*

[b] *Department of Chemistry, Orta Dogu Teknik Universitesi (ODTU/METU), Ankara 06800, Turkey*

[c] *Department of Medical Pharmacology, Gazi University, Faculty of Medicine, Ankara 06500, Turkey*

[d] *Department of Biological Sciences and Cancer Systems Biology Laboratory (CanSyl), Orta Dogu Teknik Universitesi (ODTU/METU), Ankara 06800, Turkey*

[*] Corresponding author.

E-mail address: banerjee@metu.edu.tr (S. Banerjee).

[1] Current address: Vocational School of Health Services, Department of Medical Laboratory Techniques, and Biotechnology Application and Research Center, Bilecik Şeyh Edebali University, Bilecik 11230, Turkey.

[2] Current address: University of Geneva, Faculty of Medicine, Department of Cell Physiology and Metabolism, Rue Michel-Servet 1, 1206 Genève, Switzerland.

[3] Equal contribution.

Abstract

Colloidal platinum (Pt) is widely consumed due to its health promoting benefits. However, the exact biological effects of these nanoparticles have not been studied in detail, particularly in the gut. In the present study we observed that colloidal Pt was not cytotoxic towards three different epithelial colon cancer cell lines. Co-treatment of the colon cancer cell line Caco-2 with the oxidative stress inducing agent hydrogen peroxide (H_2O_2) and colloidal Pt resulted in a significant decrease in H_2O_2 induced oxidative stress. Colloidal Pt by itself did not induce any oxidative stress. Additionally, both overnight pretreatment of

https://doi.org/10.1016/j.heliyon.2019.e01336

Caco-2 cells with colloidal Pt followed by 1 h treatment with H_2O_2, or co-treatment of cells for 1 h with colloidal Pt and H_2O_2 resulted in a significant recovery of cell death. Of note, the same protective effects of colloidal Pt were not observed when the oxidative stress was induced in the presence of 2, 2-azobis (2-amidinopropane) dihydrochloride, indicating that the source of free radicals may define the outcome of anti-oxidant activity of colloidal Pt. Colloidal Pt was also able to cross a model intestinal barrier formed *in vitro* with differentiated Caco-2 cells easily. Overall, our data indicate that colloidal Pt was not toxic towards intestinal epithelial cells, reduced H_2O_2 induced oxidative stress, protected from oxidative stress related death of intestinal epithelial cells and could pass a model gut barrier easily. Colloidal Pt can therefore be consumed orally for its anti-oxidant and other health promoting benefits.

Keywords: Molecular biology, Cell biology

1. Introduction

Platinum (Pt) is an important but non-essential metal that has found biological value as glucose sensors [1] and in cancer therapy [2]. The mode of action of platinum in cancer therapy is attributed to its ability to crosslink DNA thereby causing DNA damage and eventual apoptosis [2]. According to the Woodrow Wilson Nanotechnology Consumer Products Inventory 2011, Pt nanoparticles are some of the most commonly used nanomedicines in consumer products (http://www.nanotechproject.org/inventories/consumer/). Nanoparticles are defined as solid colloidal particles that can range in size from 10 nm to 1.0 μm [3]. Colloidal systems for dispersion of metals provide advantage of small size (1−50 nm diameter) that allows for easy absorption [4]. Platinum nanoparticles have been reported to be toxic in various model systems such as algae [5] and mammalian cells [6]. On the other hand, the size of the nanoparticle was reported to be important for bactericidal activities, with particles as low as 3 nm having strong bactericidal properties; larger particles were largely compatible with the growth of bacteria [7]. A similar size dependent effect of Pt nanoparticles in the induction of DNA damage has also been indicated [6]. Colloidal Pt suspended in hydrogen dissolved (HD) water was reported to be very effective against human tongue cancer epithelial cells by reducing cell proliferation and colony formation but had no effect on normal tongue epithelial cells [8]. Additionally, colloidal Pt was demonstrated to enhance apoptotic cell death of esophageal squamous cell carcinoma cells by sensitizing the cells to gamma irradiation [9]. Mechanistically, colloidal Pt was shown to induce apoptosis by enhancing the protein levels of p53, p21 and reducing the levels of proliferating cell nuclear antigen [10]. Furthermore, colloidal Pt nanoparticles were found to be highly hemocompatible and could enhance the fluidity of red blood cells [11].

https://doi.org/10.1016/j.heliyon.2019.e01336

Many of the beneficial effects of colloidal Pt stem from its anti-oxidant activity [11]. Superoxide anion radical ($O_2^{\cdot -}$), singlet oxygen ($^1O_2$), hydrogen peroxide (H_2O_2) and hydroxyl radical ($\cdot OH$) are typical reactive oxygen species (ROS) generated due to metabolic reactions. The reduction of oxygen to water during the production of ATP in the mitochondrial electron transport chain results in the leakage of a small number of electrons, which can directly react with oxygen to generate ROS [12]. Superoxide anion is reduced to H_2O_2 by the antioxidant superoxide dismutase (SOD), which can be transported across membranes. Although ROS are required to maintain several cellular functions including proliferation, host defense, signal transduction and gene expression [13], when steady-state ROS concentration is transiently or chronically increased, it can induce several pathological conditions such as atherosclerosis, neurodegenerative diseases and aging as well as certain types of human cancers including lung, breast, and colon cancer [14, 15]. To control the steady-state levels of ROS, cells possess finely regulated antioxidant systems: antioxidant enzymes such as SOD, catalase and glutathione peroxidase as well as endogenous and exogenous non-enzymatic small molecules including glutathione, β-carotene, vitamin C and E [16]. Colloidal Pt, due to the presence of unpaired electrons, is highly reactive and is known to exhibit intrinsic SOD/catalase-like activity by converting the superoxide radical to H_2O_2 and subsequently H_2O_2 to H_2O and O_2 under neutral and alkaline conditions [17, 18].

Platinum has also been used for a long time as colloidal dispersions; the latter was approved as a food additive of natural origin by the Ministry of Health, Labor and Welfare of Japan in 1995 [9]. Due to the size of the colloidal nanoparticles, their diffusion across the plasma membrane is unlikely [19]; although it has been shown that these particles are internalized [20], most likely through the process of pinocytosis. Several studies have shown that colloidal Pt can scavenge ROS *in vitro* [11, 18, 20], although it is not clear whether the same effect can be seen inside cells. Additionally, since colloidal Pt is approved for oral consumption, here we aimed to better establish the role of colloidal Pt on the gut. For this, we examined the effect of different concentrations of colloidal Pt on gut epithelial cells, examining its cytotoxicity, cytoprotection from oxidative stress, free radical quenching ability and passage through the gut barrier. Our data indicate that colloidal Pt is not cytotoxic, can reduce oxidative stress, and can cross the gut barrier effectively.

2. Materials and methods

2.1. Colloid Pt and its characterization

Colloidal Pt at 400 ppm concentration was provided by platinsai® (Turkey, www.londoh.co.jp). To determine whether filtration through 0.22 μm or 0.45 μm polyethersulfone (PES) filters or incubation in solution at different pH values

https://doi.org/10.1016/j.heliyon.2019.e01336

affected the size, charge or dispersion of colloidal Pt, the size distribution and zeta potential of the colloidal Pt samples were determined using a Zetasizer (NanoZS, Malvern, UK). To determine the effect of filtration, the undiluted samples were filtered through the different filters or left unfiltered and immediately measured for size and zeta potential. To determine the effect of pH on colloidal Pt, the samples were diluted 1:10 (v/v) in deionized water containing 2 g/L of NaCl (to mimic the ionic strength of gastric fluids [21]) and the pH was adjusted to 1.2, 2.0, 3.0, 4.0 and 5.0 with HCl. As a control, the colloidal Pt samples were diluted in deionized water containing 2 g/L NaCl at pH 7.5. The samples were incubated in solutions at the respective pH values for 2 h and then the size distribution and zeta potential were measured with no further modifications. The hydrodynamic diameter of colloidal Pt was reported as Z_{avg} and the zeta potential as mV. Polydispersity index (PdI) values indicated the homogeneity of the sizes of the particles. The average of 10 measurements was used for each data point.

2.2. Cell culture

Caco-2 and HT-29 cells were obtained from ŞAP Enstitüsü (Ankara, Turkey). HCT-116 cells were received from DSMZ (Braunschweig, Germany). HT-29 and HCT-116 cells were grown in RPMI-1640 without phenol red (Biological Industries, Beit Haemek, Israel) supplemented with 10% Fetal Bovine Serum (FBS) (Biological Industries, Beit Haemek, Israel, Cat. No: 04-127-1A), 2 mM L-glutamine (Biological Industries, Cat. No: 03-020-1B) and 1% penicillin/streptomycin (Biological Industries, Cat. No: 03-031-1B). Caco-2 cells were grown in EMEM-Minimum Essential Medium without phenol red with Earl's salt (Thermo Fisher Scientific, Boston, MA, USA, and Cat. No: 51200038) containing 20% FBS (Biological Industries), 1% penicillin/streptomycin (Biological Industries), 2 mM L-glutamine (Biological Industries), 1X-NEA-Non-Essential Amino Acids (Biochrom GmbH, Berlin, Germany, Cat. No: K 0293) and 1 mM Na pyruvate (Biowest, Florida, USA, cat. No: L0642-100). All cell lines were grown in a humidified atmosphere containing 5% CO_2 at 37 °C.

When the cultures reached 60−70% confluency, media were removed and the cells were washed with PBS (Dulbecco's Phosphate Buffered Saline, without Ca^{2+} and Mg^{2+}, Biological Industries, Cat. No: 02-023-1A). The cells were then detached by adding Trypsin/EDTA solution (0.25%/0.02% w/v, Biochrom GmbH, Cat. No: L2163) and incubated at 37 °C for 5 min. Finally, trypsin was inhibited with at least 3-fold of the growth media and appropriate aliquots of the cell suspension were added to new culture vessels.

2.3. Spontaneous differentiation of Caco-2 cells

Caco-2 cells were plated at high cellular density. Proliferating cells were collected the day after seeding when the cultures were 60−70% confluent (sub-confluent).

https://doi.org/10.1016/j.heliyon.2019.e01336

After about 48 hours of plating, the cells generally reached 100% confluency. To differentiate the cells, 100% confluent cells (day 0) were grown for a further 10 days [22], during which the medium was changed every other day. For every set of differentiation, the expression of sucrose isomaltase (SI) and carcinoembryonic antigen (CEA) were assayed as differentiation markers. To generate the intestinal barrier using differentiated Caco-2 cells, 6×10^5 cells were plated in Transwell inserts (Costar 0.4 μm, Corning, USA Cat. No: 3470) and grown for a further 10 days. Differentiation was confirmed by collecting the cells from the Transwells and determining the mRNA and protein expression of SI and CEA, respectively.

2.4. FITC-dextran permeability assay

To assess barrier formation in differentiated Caco-2 cells, the permeability of FITC Dextran was determined [23]. For this, Caco-2 cells were differentiated on Transwells for 10 days. FITC-dextran (FD4, Sigma Aldrich, St. Louis, Missouri, USA, Cat No: 60642-46-8) was dissolved in complete EMEM medium containing 10% FBS at 500 μg/mL concentration and then applied to the apical side of the cell monolayers on the Transwells. FD4 permeability was determined by sampling the basolateral solution for every 30 min for 3 h, while replacing the sampled amount with fresh media without FD4 at each time point. The amount of FD4 that passed the Caco-2 barrier across the Transwell membrane was quantified by fluorescence spectroscopy at 535 nm using a calibration curve using a range of concentrations of FD4 between 10 $\mu g/mL^{-1}$ mg/mL. As a control, proliferating Caco-2 cells that did not form the barrier were used.

2.5. RNA isolation, cDNA synthesis and RT-qPCR assays

Cells were collected in cell culture-grade PBS by scraping. Total RNA was isolated using an RNA Extraction Kit (NucleoSpin RNA, Macherey Nagel, Germany, Cat. No: 740955.250) according to the manufacturer's guidelines. RNA concentrations were measured with BioDrop μLITE spectrophotometer (BioDrop, Cambridge, UK). To reversely transcribe 1 μg of total RNA with random hexamers, cDNA synthesis was carried out using RevertAid First Strand cDNA Synthesis Kit (Thermo Fisher Scientific, cat no: K1622). The cDNAs were stored at −20 °C.

For RT-qPCR mixtures, 0.25 μM forward and reverse primers (shown in Table 1) and 5 μl of 2X GO Taq QPCR Master Mix containing SYBR Green (Promega, Madison, Wisconsin, USA, Cat. No: A6001) were mixed in 8 μl volume, then 2 μl of 1:20 diluted cDNA was added. β-Actin was used as an internal control. Reactions were carried out in Rotor GeneQ 6000 (Qiagen, Germany). Standard curves were prepared for each set of primers which were then used to calculate C_t values of the unknown samples. Fold changes with respect to the internal controls were

https://doi.org/10.1016/j.heliyon.2019.e01336

calculated using Pfaffl method [24]. MIQE guidelines were followed in the RT-qPCR reactions [25].

2.6. Western blotting

M-PER Mammalian Protein Extraction Buffer (Thermo Fisher Scientific, Cat. No: 78501) was used to extract proteins. Protease inhibitors (Roche, Basel, Sweden, Cat. No: 11836153001) and phosphatase inhibitors (Roche PhosStop Cat No: 4906845001) were added to the lysis buffer. After incubation on ice for 30 min, cells were centrifuged at 14000 × *g* for 10 min; then supernatants containing the total protein lysate were collected in fresh eppendorf tubes. Protein concentration was determined using Coomassie Protein Assay Reagent (Thermo Fisher Scientific, Cat. No: 23200) by reference to a standard curve generated with known concentrations of BSA (Bovine Serum Albumin).

For the separation of proteins by SDS-PAGE, the proteins were boiled at 95 °C for 6 min in a 6X loading dye (12% SDS, 30% β-mercaptaethanol, 30% glycerol, 0.02% bromophenol blue, 375 mM Tris−HCl pH 6.8). Electrophoresis was carried out at 100 V using 10% SDS-polyacrylamide gels loaded with equal amounts of protein (20 μg). For the transfer of proteins onto polyvinylidene fluoride membranes (Roche, Cat no: 3010040001), wet transfer was performed with constant current at 380 mA, 115 V for 75 min. The membranes were blocked by using 5% skim milk (Sigma Aldrich) in 1X TBS containing 0.1% Tween-20 (Applichem, Germany) for 1 h at room temperature on a shaker. Membranes were incubated with primary antibodies at 4 °C overnight on a shaking platform. Next day, membranes were washed with TBS-T, followed by incubation with horseradish peroxidase-conjugated secondary antibody for 1 h at room temperature, on a shaker. List of primary and secondary antibodies are given in Table 2. Visualization of the blots was performed using WesternBright ECL HRP substrate (Advansta, Menlo Park, CA, USA) and imaged on a Chemi-Doc MP (Bio-Rad, Hercules, CA, USA).

Table 1. Primer sequences used in RT-qPCR and their properties.

Name	Primer sequences (5′-3′)	Annealing temperature (°C)	Product size (bp)	Target mRNA ID
Sucrase isomaltase (SI)	Forward: CAAATGGCCAAACACCAATG Reverse: CCACCACTCTGCTGTGGAAG	59	160	NM_001041.3
β-Actin	Forward: CAGCCATGTACGTTGCTATCCAGG Reverse: AGGTCCAGACGCAGGATGGCATG	60	151	NM_003900.4

https://doi.org/10.1016/j.heliyon.2019.e01336

2.7. Determination of cell viability

The colloidal Pt sample was filtered through a 0.22 μM PES filter for sterilization. Vybrant® MTT (3-(4, 5-dimethylthiazol-2-yl)-2, 5-diphenyltetrazolium bromide) Cell Proliferation Assay (Life Technologies, Carlsbad, CA, USA, Cat. No: M6494) was used for determination of cell viability of Caco-2, HCT-116 and HT-29 cell lines in the presence of different concentrations of colloidal Pt. First, 5×10^3 cells per well were plated in 96-well plates in their corresponding growth medium. Cell proliferation was determined under the following conditions:

1. Treatment with colloidal Pt only (1%−20% v/v diluted in the corresponding cell culture medium) for 48 h to determine the effect of colloidal Pt on cell viability.
2. Treatment first with 20% colloidal Pt for 24 h then 1 h with 250 μM-5 mM H_2O_2 (Sigma-Aldrich, Cat No: 216763) after removal of Pt containing growth medium.
3. Co-treatment with Pt (20%) and H_2O_2 or co-treatment with Pt (20%) and 5 mM-80 mM 2, 2-azobis (2-amidinopropane) dihydrochloride (AAPH, dissolved in dH_2O, Sigma-Aldrich, Cat. No: 440914) for 1 h.

Following the treatments, the medium was removed and the MTT cell viability assay was carried out according to the manufacturer's instructions. Briefly, 12 mM MTT stock solution was diluted with growth medium in 1:10 ratio and distributed to each well as 100 μl. Empty wells containing only 100 μl of diluted MTT were used as blank. The plates were incubated at 37 °C for 4 h. In order to dissolve the formazan crystals, 100 μl of 1/10 (g/mL) SDS/dH_2O (containing 0. 01 N HCl) solution was added for each well followed by incubation at 37 °C for 16 h. Finally, measurements were taken at 570 nm in MultiSkan GO Microplate Spectrophotometer (Thermo Scientific) microplate reader. Sterile dH_2O was used as vehicle in colloidal Pt and AAPH treatments. Experiments were carried out with at least two biological replicates each with eight technical replicates.

Table 2. List of the antibodies and conditions for western blot.

Antibodies	Source	Dilutions
β-Actin	Santa Cruz Biotechnology, Cat. No: sc-47778	1:4000 in 5% skim milk in TBS-T
Mouse anti-CEA (Clone Col1)	Invitrogen Cat. No: 180057	1:500 in 5% skim milk in TBS-T
Goat anti-rabbit IgG HRP	Advansta Cat. No: R-05072-500	1:4000 in 5% skim milk TBS-T
Goat anti-mouse IgG HRP	Advansta Cat. No: R-05071-500	1:4000 in 5% skim milk TBS-T

https://doi.org/10.1016/j.heliyon.2019.e01336

2.8. Determination of oxidative stress: dihydroethidium (DHE) staining assay

In the presence of free radicals, oxidization of DHE that normally exhibits blue fluorescence in the cytosol results in the intercalation of DNA and formation of red fluorescence in the nucleus, which can then be measured by flow cytometry [26]. Caco-2 cells were treated with either 20% (v/v) colloidal Pt or 500 μM H_2O_2, or co-treated with 20% (v/v) colloidal Pt and 500 μM H_2O_2 for 1 h. Cells (5×10^5) were trypsinized, washed with PBS and centrifuged at 400 × *g* for 7 min and the pellets were resuspended in 0.5 mL DHE (Thermo Fischer Scientific, Cat. No: D1168) staining solution (3.2 μM in 1X cell culture grade PBS). The samples were incubated for 20 min at 37 °C in dark and then analyzed in a BD Accuri C6 Flow cytometer (Becton-Dickinson, Franklin Lakes, New Jersey, USA) in FL-2 channel immediately.

2.9. Inductively coupled plasma mass spectrometry (ICP-MS)

To determine the amount of colloidal Pt that can cross the Caco-2 barrier (mimicking the intestinal barrier function [27]) ICP-MS (Thermo Scientific X series) with a concentric nebulizer and Peltier effect cooled spray chamber was used. Caco-2 cells (6×10^5) were seeded on Transwells and differentiated for 10 days. After differentiation, growth medium containing 20% (v/v) colloidal Pt was added to Transwells inserts. After 3 h, samples were collected from both the apical and basolateral side of the differentiated cells and subjected to ICP-MS. The permeability of the differentiated Caco-2 cells to colloidal Pt was compared to the permeability of sub-confluent Caco-2 cells.

Instrumental working parameters were optimized using "Tune A" mixed standard solution with a concentration of 10 μg/L for each element as suggested by the manufacturer. Tune A solution contains Li(I), Co(II), In(III), Pb(II), Bi(V) and U(IV) ions in 0.5 mol/L nitric acid solution. Continuous flow mode with 100 ms dwell time was used for Pt determination. Performance of the instrument was regularly monitored using this solution; if there was a change in the instrument sensitivity with time, autotune sequence was run again. Furthermore, a fine tuning of the target isotopes was performed using 10 μg/L Pt solution. The calibration graph for Pt is shown in Fig. 1. Quantification was carried out with ^{194}Pt, ^{195}Pt and ^{196}Pt isotopes. Plasmalab and Microsoft Excel software were used for evaluation of the data.

2.10. Statistical analyses

Results are expressed as the mean ± standard error of mean (SEM). Data analyses and graphing were carried out with Graphpad Prism 6.0. t-test was used for statistical analysis, and differences at $p \leq 0.05$ were considered significant (*$p \leq 0.05$; **$p \leq 0.01$; ***$p \leq 0.001$; ****$p \leq 0.0001$).

https://doi.org/10.1016/j.heliyon.2019.e01336

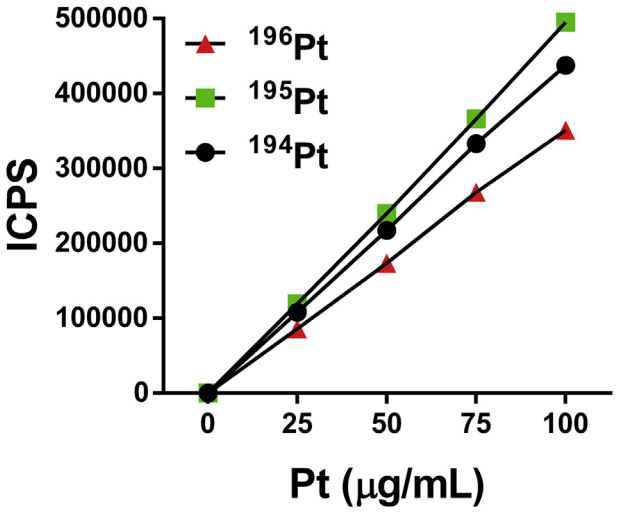

Fig. 1. Calibration graph and the best line equation for ^{194}Pt, ^{195}Pt and ^{196}Pt isotopes by ICP-MS.

3. Results and discussion

3.1. Characterization of colloidal platinum nanoparticles

We first determined whether sterilization of colloidal Pt by filtering with 0.22 μm or 0.45 μm filters affected the size of the colloidal Pt nanoparticles by using dynamic light scattering (DLS) (Fig. 2). This is a technique for understanding the diffusion behavior of macromolecules in solution, thus, this behavior is affected by the size and shape of macromolecules [28]. The size of the colloidal Pt was calculated as 7.4 nm ± 0.08, 8.1 nm ± 0.14 and 8.9 ± 0.22 for unfiltered, 0.45 μm and 0.22 μm filtered samples, respectively at 25 °C. The results show a slight variation in the hydrodynamic size of the particles before and after filtration (Fig. 2). These variations may have resulted from the dynamic nature and rapid movement of the very small particles medium resulting in a fluctuating intensity signal [29]. It should also be kept in mind that this is the hydrodynamic size that includes layer of water around the nanoparticles. It is likely that the actual size of the particles is lower. For all future experiments, the colloidal Pt was filtered through a 0.22 μm filter for sterilization. Additionally, the zeta potential for the 0.22 μm filter sterilized sample was determined as -29 mV while the zeta potential of the unfiltered sample was −28.1 mV indicating filtration did not have any impact on the electric charge around the surface of the particles.

To determine the stability of colloidal Pt at different pH values (1.2, 2.0, 3.0, 4.0, and 5.0), we have resuspended the colloidal Pt solution at 10 % (v/v) in deionized water and 2 g/L NaCl and adjusted the pH with HCl. As a control we used deionized water containing 2 g/L NaCl at pH 7.5. We observed that at pH 1.2, 2.0 and 3.0 the colloidal Pt underwent aggregation and precipitation, which was manifested in a dramatic increase in the hydrodynamic size of the colloidal particles at these pH values

https://doi.org/10.1016/j.heliyon.2019.e01336

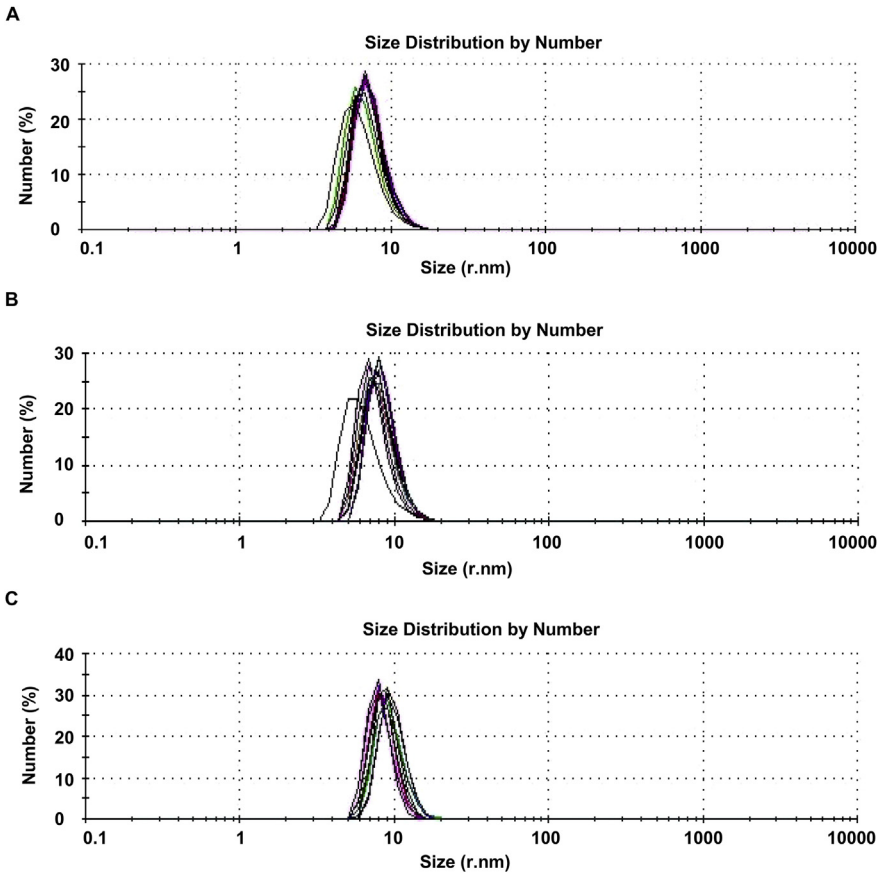

Fig. 2. Characterization of colloidal platinum nanoparticles. Intensity particle size (radius in nm-r.nm) distribution, obtained by the Dynamic Light Scattering (DLS, Malverin Zeta Sizer, 135° backscatter), for unfiltered (A), 0.22 μm (B), 0.45 μm (C) filtered colloidal Pt samples are shown. The data were collected 10 times for each sample.

(Table 3). We also measured the zeta potential of the samples at the different pH values and observed a decrease in the zeta potential of the samples at the lower pH values.

Generation of a colloidal solution requires a high input of energy that is likely to push these systems far from equilibrium [30]. The colloidal structure consists of two continuous phases that can exhibit phase transitions manifested by sudden changes in parameters such as temperatures and/or concentrations [30]. It is possible that the colloidal system in the Pt solution got protonated at the lower pH values, which may have resulted in more positive charges on the particles and thereby aggregation and precipitation. This can also be seen from the zeta potential of the samples that changed from −28 mV when incubated in water at pH 7.5 to significantly more positive values at the lower pHs. However, it is difficult to determine the precise mechanism of the aggregation at the critical pH value of 3 without having exact knowledge of the chemical composition of the surfactant found in the colloidal Pt solution; this data is unavailable to the public.

https://doi.org/10.1016/j.heliyon.2019.e01336

Table 3. Hydrodynamic size and zeta potential of colloidal Pt at different pH values. The pH of the solution was adjusted with HCl (except the control at pH 7.5). All solutions contained 2 g/L NaCl and all solutions were incubated for 2 h at 37 °C.

pH	Hydrodynamic size (nm)	Zeta potential (mV)
1.2	500 ± 59.2	−12.9 ± 1.8
2.0	470.7 ± 58.9	−11.3 ± 2.1
3.0	485.1 ± 60.8	−15.2 ± 1.2
4.0	7.8 ± 0.3	−17.4 ± 3.1
5.0	7.2 ± 0.5	−12.0 ± 0.5
7.5	7.6 ± 0.4	−28.7 ± 1.3

It is well known that the pH of the gastric fluid in healthy subjects is in the range of 1.3−2.5 during fasting [31]. However, after eating, the pH can increase to a range of 4.5−5.8. Around 1 h after eating, the pH of the stomach can decrease to less than 3.1 [31]. Thus, it is likely that if consumed with food rather than on an empty stomach, the colloidal Pt solution will be in an environment with a higher pH value at which it is more stable.

We also determined the pH of 1%−20% (v/v) colloidal Pt samples diluted in cell culture medium using a pH meter. Colloidal Pt itself was acidic (pH: 4.86), while the pH of the cell culture medium was 8.73. The pH of the cell culture medium containing colloidal was 8.73 for every dilution used, indicating that the presence of colloidal Pt did not change the pH of the culture medium.

3.2. Effect of colloidal platinum on cell viability

In order to assess the effect of the colloidal platinum on cell viability, an MTT assay was carried out with HCT-116, Caco-2 and HT-29 cell lines. 20% (v/v) colloidal Pt (corresponding to 80 ng/μl colloidal Pt) was the maximum concentration that was used since more than 20% (v/v) vehicle (dH_2O) in the control wells decreased the number of viable cells. Cell viability remained unaffected at all doses of colloidal Pt in three different CRC cell line models (Fig. 3). Attempts to concentrate the colloidal Pt using a Speedvac (Thermo Scientific) to achieve higher treatment concentrations resulted in a loss of the colloidal nature of the solution.

Pt based drugs such as cisplatin, oxaliplatin and carboplatin are widely used as chemotherapy drugs [32]. Although Pt as a metal is highly inert, these drugs contain Pt (II) that is known to be highly active as it can accept two electrons [33]. The primary mechanism of action of these compounds includes formation of adducts with DNA that create bulky lesions and therefore inhibit transcription by RNA polymerase II. If the damage is extensive and cannot be repaired by DNA repair pathways,

https://doi.org/10.1016/j.heliyon.2019.e01336

the cell undergoes apoptosis [34]. Colloidal Pt, consisting of a colloidal dispersion of the metal, needs to be stabilized to prevent aggregation; this in turn involves capping of the active sites, leading to lower reactivity [33]. Additionally, colloidal metal solutions by definition have neutral metal atoms; although based on the isoelectric point of platinum (2.8), the solution at pH 4.9 is likely to have a negative charge [35]. Li et al. reported that colloidal Pt showed considerable toxicity towards the esophageal squamous cell carcinoma cell line KYSE-70, which was further enhanced in the presence of gamma irradiation [9]. These authors used 0, 50 and 100 ppm colloidal Pt, with nearly 50% reduction in cell viability and approximately 40% increase in apoptosis reported with 100 ppm colloidal Pt when compared to untreated cells. In the current study, we have used 80 ppm colloidal Pt as the maximum concentration but have observed minimal cell death in three different epithelial cancer cell lines. The surface reactivity of platinum nanoparticles is dependent on size; larger particles with lower work function or those particles with enhanced O_2 chemisorption show greater catalytic activity [36]. On the other hand, in biological systems, colloidal Pt with smaller particle sizes (around 3 nm) were reported to show greater toxicity [7]. In the current study, the hydrodynamic size of the colloidal particles was between 7 nm and 8 nm. It is possible that the size of the colloidal particles used in the current study was not toxic to the cells.

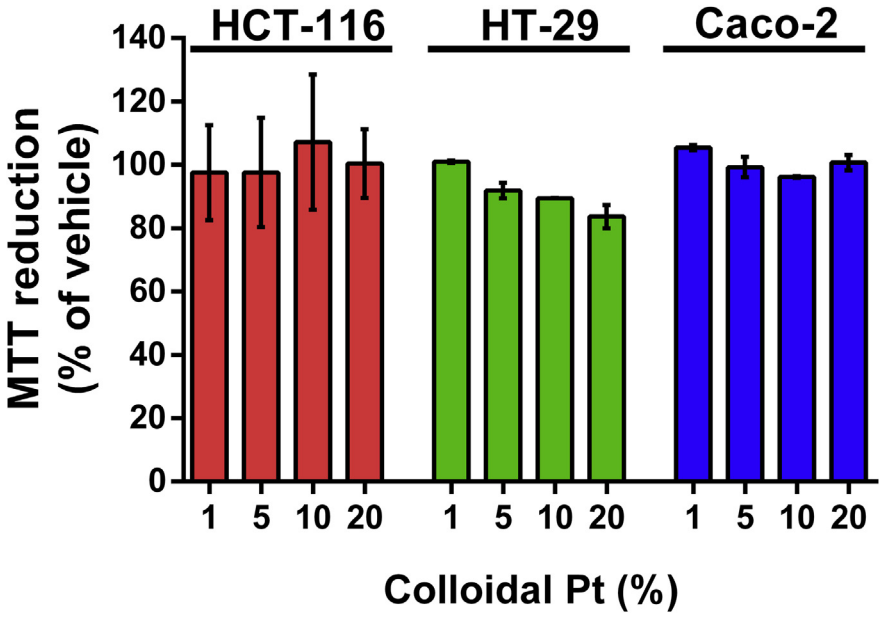

Fig. 3. Effect of colloidal platinum on cell viability. HCT-116, Caco-2 and HT-29 cells were treated with 1%−20% (v/v) colloidal Pt for 48 h, then MTT assay was carried out. Percent viable cells normalized to their corresponding vehicle treated control cells are shown. The experiment was carried out with at least 2 independent biological replicates, each containing 8 technical replicates.

https://doi.org/10.1016/j.heliyon.2019.e01336

3.3. Effect of colloidal Pt on the generation of Reactive Oxidative Species (ROS)

Colloidal Pt has been previously reported to protect from oxidative stress [11]. To determine whether the same could be seen in the CRC cell lines used, a Dihydroethidium (DHE) assay was used. DHE is a membrane permeable dye used extensively for monitoring superoxide production [37]. Caco-2 cells were first treated with 500 μM H_2O_2 for 1 h to induce ROS production; some of the cells were co-treated with 500 μM H_2O_2 and 20% (v/v) colloidal Pt for 1 h, followed by the DHE assay. We observed low ROS production in Caco-2 cells treated with colloidal Pt sample or vehicle control (Fig. 4, 17.5% DHE stained cells), showing that colloidal Pt by itself did not result in ROS production and oxidative stress. More importantly, we observed a nearly 50% decrease in ROS production (Fig. 4, 23.6% DHE stained cells) in Caco-2 cells co-treated with colloidal Pt and H_2O_2 as compared to cells treated with H_2O_2 alone (Fig. 4, 78.4% DHE stained cells). This suggests that treatment of cells with colloidal Pt may relieve H_2O_2 triggered oxidative stress.

The decomposition reaction H_2O_2 with Pt as a catalyst was reported to be a two-step process as shown below:

$$\begin{array}{l}(\text{Step 1})Pt + H_2O_2 \rightarrow H_2O + Pt(O) \\ \underline{(\text{Step 2})Pt(O) + H_2O_2 \rightarrow Pt + O_2 + H_2O} \\ \text{Overall}: \ 2H_2O_2 \rightarrow O_2 + 2H_2O\end{array}$$

The first and rate determining step includes adsorption of H_2O_2 on oxide-free Pt and the decomposition of H_2O_2 into water and oxidized Pt(O) (Step 1). The next step (Step 2) is initiated due to the instability of the oxidized Pt, which promotes the decomposition of H_2O_2 further into H_2O and O_2 [36].

In the current study, a mixture of colloidal Pt and H_2O_2 led to the formation of bubbles in the culture medium indicating that the steps described above were most likely occurring. Thus, the decomposition of H_2O_2 into water and oxygen ameliorated H_2O_2 mediated ROS formation in the cells as shown in Fig. 4.

3.4. Effect of ROS generators with colloidal platinum nanoparticles on cellular viability

We next wanted to determine whether amelioration of oxidative stress in the presence of colloidal Pt could also affect cell proliferation. For this, we either co-treated Caco-2 cells with colloidal Pt and 2, 2-azobis (2-amidinopropane) dihydrochloride (AAPH) or with colloidal Pt and H_2O_2. H_2O_2 is a source of reactive oxygen species (ROS). ROS are chemically-reactive molecules containing oxygen, including superoxide anions or singlet oxygen and their production is catalyzed

https://doi.org/10.1016/j.heliyon.2019.e01336

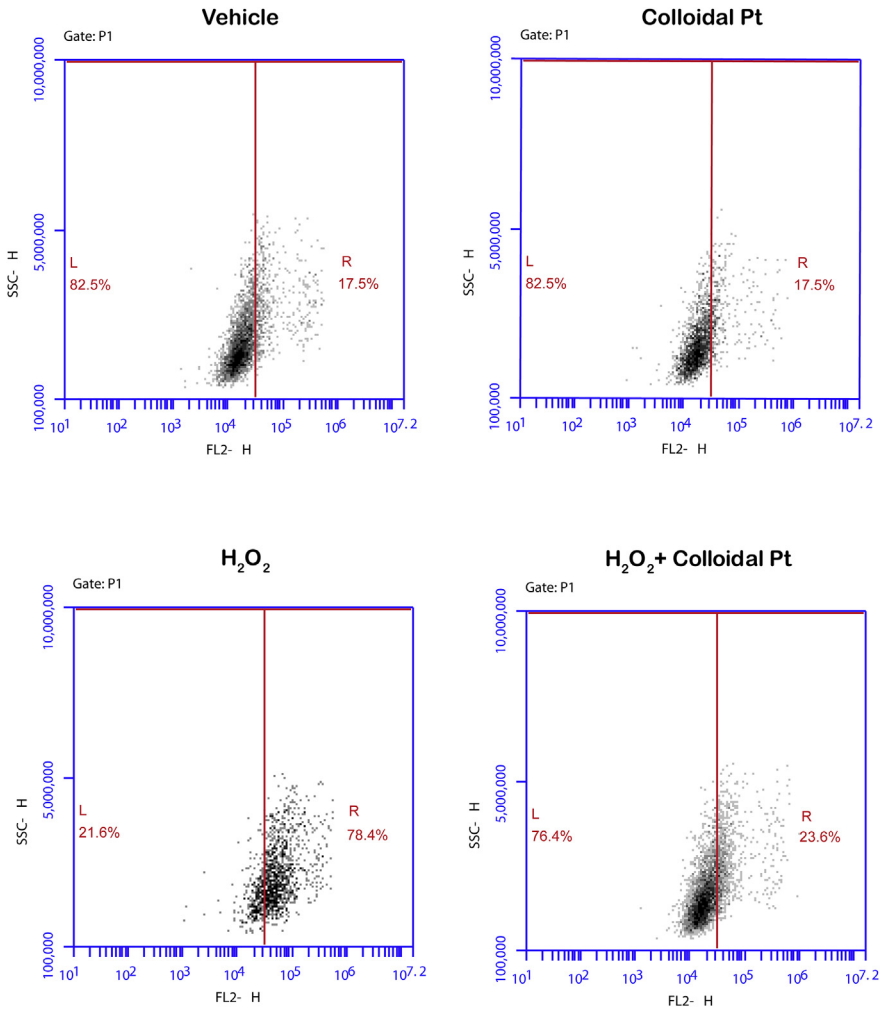

Fig. 4. Effect of colloidal Pt nanoparticles on the production of reactive oxidative species (ROS). Caco-2 cells were treated with only 20% (v/v) colloidal Pt or only 500 μM H_2O_2, or with a combination of 500 μM H_2O_2 and 20% (v/v) colloidal Pt for 1 h. 20% (v/v) dH_2O treatment was used as vehicle. The production of ROS was determined by the DHE staining using flow cytometry. Representative flow cytometry dot plots of two independent experiments are shown.

by oxidative enzymes in cell membranes, mitochondria, peroxisomes and endoplasmic reticulum [38].

To determine whether pretreatment of Caco-2 cells with colloidal Pt could protect against H_2O_2 induced cell death, Caco-2 cells were co-treated with 20% (v/v) colloidal Pt and H_2O_2 (250 μM-5 mM) for 1 h. In another experimental set-up, the cells were treated with 20% (v/v) colloidal Pt for 24 h first; then, colloidal Pt was removed, the cells were washed and treated with H_2O_2 (250 μM-5 mM) for 1 h and assayed for cell viability. As can be seen in Fig. 5A and B, H_2O_2 treatment of Caco-2 cells resulted in nearly 50% cell death as expected. However, co-treatment of Caco-2 cells with H_2O_2 and colloidal Pt resulted in a complete recovery

https://doi.org/10.1016/j.heliyon.2019.e01336

in cellular viability (Fig. 5A). This was most likely due to the chemical decomposition of H_2O_2 into O_2 and H_2O in the presence of Pt. Pre-treatment with colloidal Pt followed by H_2O_2 treatment was also found as protective against H_2O_2 mediated cytotoxicity but to a lesser extent than colloidal Pt and H_2O_2 co-treatment (Fig. 5B). Collectively, these results suggest that colloidal Pt could reduce H_2O_2-mediated cytotoxicity in target cells; more importantly, cellular viability was preserved even when the cells were pretreated with colloidal Pt followed by treatment with only with H_2O_2, suggesting that colloidal Pt could inhibit oxidative stress related cell death. To explain the mechanism behind the observation that pretreatment of cells with colloidal Pt could protect from H_2O_2 induced cell death, it has been suggested that Pt can act as a superoxide dismutase/catalase mimetic [39, 40] whereby it can reduce the formation of superoxides and reduce the expression and activity of apoptosis related proteins such as caspase 3 and Bid [40].

Oxidative stress can result in cellular and structural damage that may affect membrane, proteins, lipids and DNA; thereby affecting cellular proliferation and gene expression [41]. Most of biological sources of H_2O_2 demand the spontaneous or catalytic breakdown of superoxide anions ($O^{\cdot-}$) which is produced by the partial reduction of oxygen during aerobic respiration. H_2O_2 can also be produced extracellularly for instance by the immunoglobulin G-catalyzed oxidation of water, by receptor/ligand interactions (for example in response to growth factors), and by phagocytic immune cells [42] and can enter cells by simple or facilitated diffusion [43]. H_2O_2 is involved in normal cellular metabolism at low concentrations as a metabolite from non-enzymatic and superoxide dismutase-catalyzed reactions and under normal conditions it is rapidly neutralized in tissues by anti-oxidant defense systems [41]. It is one of the key molecules in the redox cycle in which it can act as a messenger to carry the redox signal to the target site [41]. Additionally, it can be converted to reactive hydroxyl radicals (HO●) with Fenton reaction, which then can react with biological molecules to accept a hydrogen atom. When iron salt containing foods are ingested frequently, it can lead to the formation of hydroxyl radicals via the Fenton reaction. In this case, the main target organ is the gastrointestinal (GI) tract where iron absorption primarily occurs. Moreover, it has been shown that high concentrations of H_2O_2 can affect cell membrane dynamics and disrupt membrane permeability, which can result in cell death eventually [41, 44]. Besides, Rao et al. showed that H_2O_2 induces impairment of the intestinal epithelial barrier function by disrupting paracellular junctional complexes [45]. Therefore, protective action of colloidal Pt against detrimental effects of H_2O_2 may contribute to the proper maintenance of tissues.

The recommended dose for colloidal Pt from the vendor's webpage (platinsai) is 5 mL per day (https://www.londoh.co.jp/en/products/sai/index.html). Based on the concentration of Pt in colloidal Pt (400 ppm), the amount of Pt recommended per day in colloidal form is about 2 mg. In an average individual with 5 L of blood,

https://doi.org/10.1016/j.heliyon.2019.e01336

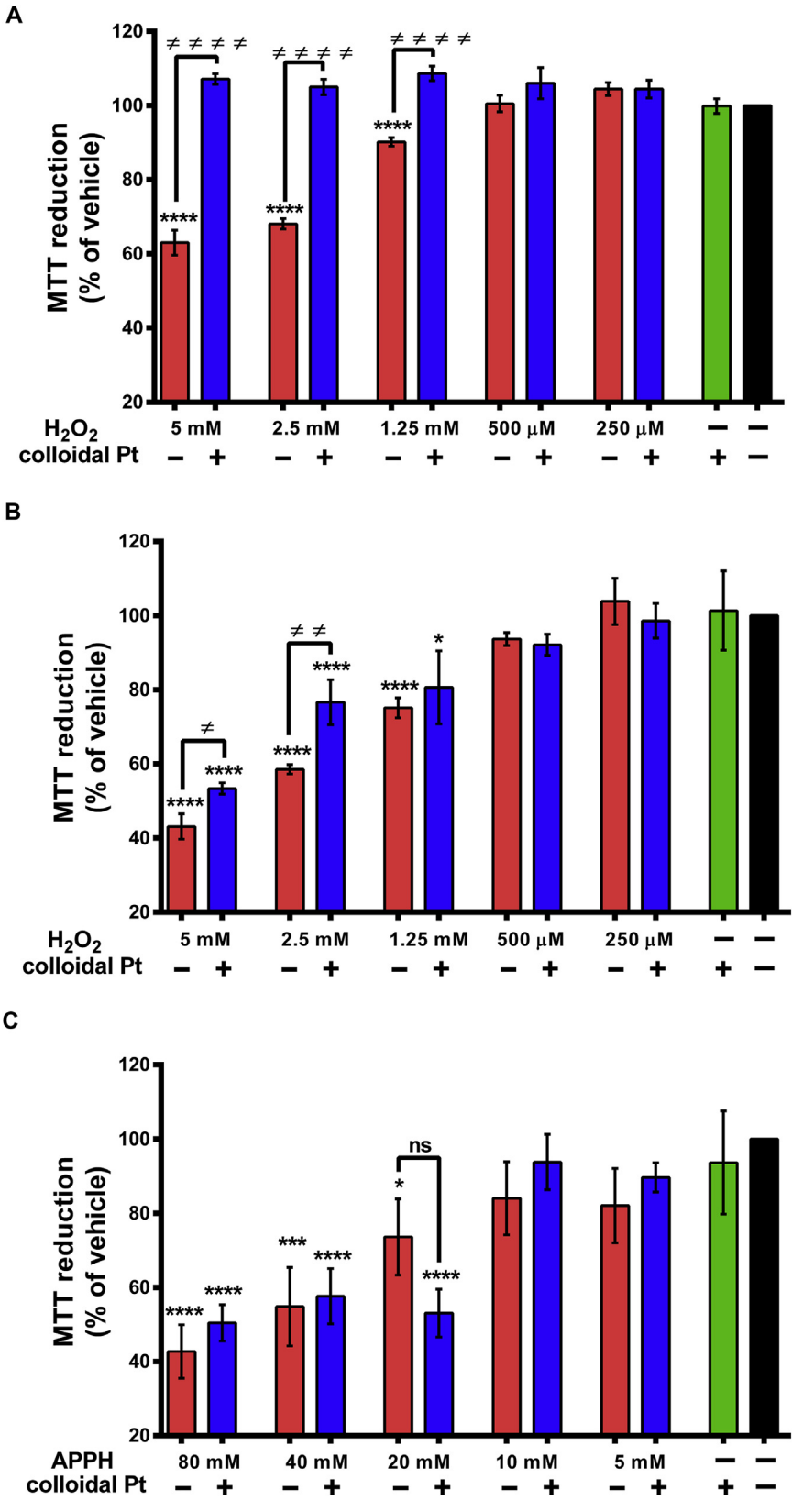

https://doi.org/10.1016/j.heliyon.2019.e01336

this would amount to a plasma concentration of around 0.4 ppm, assuming 100% absorption in the gut. In the current study, up to 80 ppm colloidal Pt was used, which is nearly 200 times higher than the recommended amount of colloidal Pt. The concentration of hydrogen peroxide (H_2O_2) in blood and plasma is unclear. Forman et al. have stated that human blood H_2O_2 levels range from a possible low of 0.25 μM to a probable normal range of 1−5 μM [46]. In the current manuscript, we used a range of 5−0.25 mM of H_2O_2 and observed that concentrations of 1.25 mM and higher were highly toxic to the cells, which is 250 folds higher than the normal range of H_2O_2 in blood. Therefore, when compared to estimated physiological ranges, both colloidal Pt and H_2O_2 were used in excess in this study. Nonetheless, the ratio of the Pt amount and H_2O_2 concentration are comparable (human body: 2 mg Pt/5 μM H_2O_2; experimental, *in vitro*: 400 mg Pt/1250 μM H_2O_2).

We next wanted to determine whether colloidal Pt would have a similar cytoprotective effect on cells treated with a different source of ROS such as AAPH. However, when we treated Caco-2 cells with both AAPH and colloidal Pt, we did not observe any recovery in cell viability compared to AAPH treated cells alone (Fig. 5C). These observations may have resulted from differences in the mode of action of H_2O_2 and AAPH. AAPH, a water soluble compound, is responsible for the generation of alkyl radical (R■), which in the presence of oxygen is converted to the corresponding peroxyl radicals (ROO■). AAPH therefore can induce lipid peroxidation, which may then lead to formation of different hydroperoxides depending on reaction conditions [47]. Additionally, these peroxyl radicals can result in further oxidization of polyunsaturated fatty acid (PUFA) molecules, causing new chain reactions to produce more radicals [48]. On the whole, because of the sophisticated nature of ROS biology including different expression profiles of oxidative versus anti-oxidative enzymes, their subcellular locations, and the types of the substrates for these enzymes may have resulted in different results in these assays.

3.5. Caco-2 cell line model of intestinal barrier

The gastrointestinal barrier is formed of a single layer of cells connected by junctional proteins that plays an important role in the protection of the internal environment from many ingested toxins, food contaminants and bacteria; the barrier also

Fig. 5. Effect of ROS generators with colloidal platinum nanoparticles on cell viability. A. Caco-2 cells were co-treated with 20% (v/v) colloidal Pt and 250 μM-5 mM H_2O_2 for 1 h, B. Caco-2 cells were treated first with 20% (v/v) colloidal Pt for 24 h, then colloidal Pt was removed and cells were washed and then treated with 250 μM-5 mM H_2O_2 for 1 h, C. Caco-2 cells were co-treated with 20% (v/v) colloidal Pt and 5 mM-80 mM 2, 2-azobis (2-amidinopropane) dihydrochloride (AAPH) for 1 h, then MTT assay was carried out. The experiment was carried out with at least two independent biological replicates, each containing 8 technical replicates. The statistical analyses were performed using t-test. For the statistical analysis, "*" stands for comparing with "vehicle", "≠" stands for comparing with the corresponding treatment.

https://doi.org/10.1016/j.heliyon.2019.e01336

helps in the rapid absorption of electrolytes and water via paracellular movement [49]. The Caco-2 cell line is a very well established *in vitro* model, which when spontaneously differentiated, mimics small intestinal cells in which the monolayer can show brush border microvilli, tight junctions, and dome formation [27]. In the current study, we differentiated Caco-2 cells on Transwells for 10 days to establish a polarized differentiated cells layer containing an apical and a basolateral side. Intestinal barrier formation was confirmed by determining the flux of 4 kDa FITC-dextran (FD). As expected, there was a significant decrease in the permeability of FD in differentiated cells because of the barrier formation when compared with the sub-confluent cells (Fig. 6A). The flux was determined with the help of a standard curve generated with known amounts of FD4 (Fig. 6A, right panel).

To further establish the differentiation of the cells (and thereby the establishment of a barrier) we determined the expression of sucrose isomaltase (SI), an enzyme that is highly expressed in small-intestinal enterocyte-like cells [50]. High expression of SI is a marker of differentiation in Caco-2 cells [22]. Human carcinoembryonic antigen (CEA), another differentiation marker for Caco-2 cells, is a cell surface glycoprotein and an important intercellular adhesion molecule [51]. As compared with the proliferating cell control (sub-confluent cells), Caco-2 cells differentiated in the Transwells exhibited significantly higher expression of both SI and CEA (Fig. 6B and C; Supplementary Fig. 1).

3.6. Effect of colloidal Pt nanoparticles on Caco-2 intestinal barrier model

After establishing the 3D *in vitro* intestinal barrier in Transwells, we next wanted to determine whether the colloidal Pt nanoparticles could easily cross the barrier. This data is important in establishing whether colloidal Pt can be used as a health supplement. Complete medium containing 20% (v/v) colloidal Pt was added to the upper chamber (representing the apical border of the membrane) of both differentiated and sub-confluent state cells. After 3 h, media from both the upper chamber and the lower chamber (representing the basolateral pole) were collected and subjected to ICP-MS to determine the Pt levels. The Pt ratio determined in the apical to basolateral regions was slighly higher in the differentiated cells compared to proliferating cells, although the difference was not statistically significant (Fig. 7A and B). Based on these experiments it is possible to conclude that colloidal Pt is capable of crossing the intestinal barrier. Passage of drugs/supplements across the intestinal barrier is a determinant of oral bioavailability [52]. Particles can pass the intestinal barrier either through transcytosis or in a paracellular manner. Transcytosis can be via endocytosis, an energy dependent process that includes clathrin-mediated endocytosis, caveolae mediated endocytosis, macropinocytosis and phagocytosis, or via energy independent non-endocytic pathways [53]. Previous studies have shown that

https://doi.org/10.1016/j.heliyon.2019.e01336

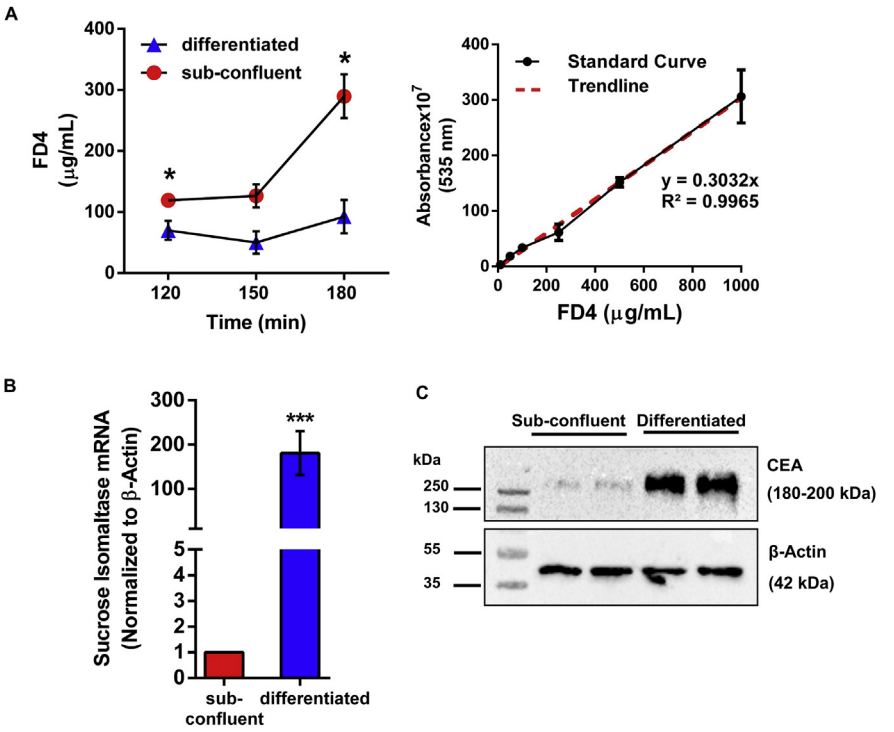

Fig. 6. *In vitro* Caco-2 cell line model of intestinal barrier. A. Caco-2 cells were grown on Transwells and differentiated for 10 days to form an intestinal barrier. Intestinal barrier formation was confirmed by determining the flux of FITC-dextran (FD) (on the left). Serially diluted FD was used to establish a standard curve (on the right). In all of the experiments, proliferating state sub-confluent cells were used as controls. Two independent biological replicates each with three technical replicates were used in this assay. B. qRT-PCR analysis of Sucrose Isomaltase (SI) mRNA levels was shown in differentiated versus proliferating (sub-confluent) cells. β-Actin mRNA levels were used for normalization. t-test was used to compare the means. C. Western blot analysis of carcinoembryonic antigen (CEA) is shown. β-Actin served as a loading control. For full non adjusted images of the Western blots please see Supplementary Fig. 1.

colloidal gold nanoparticles could be transcytosed by microfold (M) cells but could not cross the Caco-2 model of intestinal epithelial barrier in a paracellular manner [54]. Lipid nanoparticles have been shown to be transported across a Caco-2 barrier within 4 h preferentially by clathrin mediated endocytosis [52]. In the current study it appears that colloidal Pt could easily pass the intestinal barrier. It is possible that the particles were engulfed by the cells and then transported to the basolateral surface, ensuring oral bioavailability of the nanoparticles. After entry, most nanoparticles are trafficked along the endolysosomal pathway involving proteins such as Rab7a, Rab9a and Lamp1 which guide the vesicles to the lysosome for degradation or storage [55]. A portion of the endocytosed nanoparticles can also be trafficked for transcytosis for exit from the cells, most likely involving vesicle proteins such as Rab27a that is defined as an exocytotic marker [55]. While many nanoparticles are trafficked in this manner through the cells, future studies will indicate whether colloidal Pt is also trafficked by the same mechanism.

https://doi.org/10.1016/j.heliyon.2019.e01336

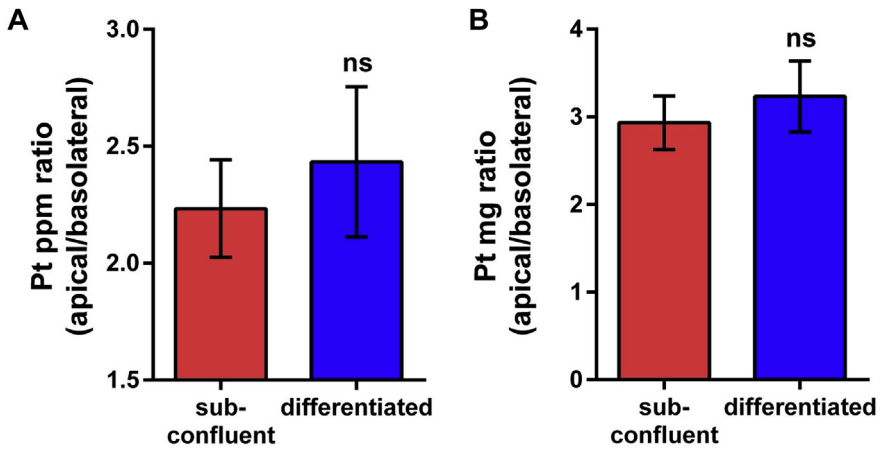

Fig. 7. Effect of colloidal Pt on Caco-2 intestinal barrier model. Caco-2 cells were differentiated on Transwells for 10 days after which complete medium containing 20% (v/v) colloidal Pt was added to the upper chamber of the Transwells in both differentiated and proliferating (sub-confluent) cells. After 3 h, the medium was sampled from both the apical and the basolateral regions (upper and lower chambers of the Transwell respectively) and subjected to ICP-MS to determine the Pt levels. Calculations were carried out accoring to a calibration curve shown in Fig. 1. The amount of Pt was determined as parts per million (ppm) and mg and the ratio of the Pt determined in the apical/basolateral sides are shown in the graphs. This assay was conducted as three independent biological replicates. t-test was used as the statistical method.

4. Conclusions

Nanoparticles (NPs) have one dimension that measures less than 100 nm at least. The properties of many conventional metals can change when formed from nanoparticles [56]. In particular, colloidal Pt NPs can possess a broad range of properties that make them convenient for many practical applications in fields such as nano-catalysts, electrical conductivity, optics, and for specific biomedical purposes such as implant coatings, imaging agents, diagnostics, drug delivery systems [57, 58]. Pt NPs are usually used in the form of colloid or suspension in a fluid [59]. A colloid is technically defined as a stable dispersion of particles in a fluid medium [60]. In this work, we investigated the cytotoxic effect as well as protective effects of colloidal Pt on oxidative stress.

We first analyzed the effect of colloidal Pt on cellular viability and found that colloidal Pt was not toxic to three different epithelial cell lines originating from the colon. Next, we examined the cellular response to oxidants in the presence of colloidal Pt. We found that colloidal Pt notably decreased H_2O_2 triggered ROS production in Caco-2 human epithelial colorectal adenocarcinoma cells. Moreover, our results indicate that colloidal Pt can protect epithelial cells from oxidative stress induced cell death irrespective of whether it was co-treated or pre-treated with H_2O_2. On the other hand, we did not observe any protective effect of colloidal Pt against AAPH induced oxidative stress mediated toxicity in Caco-2 cells. In addition to these features, as a measure of oral bioavailability, we also asked if colloidal Pt

https://doi.org/10.1016/j.heliyon.2019.e01336

was able to pass through the intestinal barrier. Using a Transwell model of intestinal barrier generated from differentiated Caco-2 cells, we demonstrated that colloidal Pt could effectively cross intestinal epithelial barrier. H_2O_2 is known to disrupt the intestinal barrier. Disruption of this barrier facilitates translocation of harmful substances and pathogens to the bloodstream by enhancing intestinal permeability. An extensive number of pathologies and diseases, such as infections with intestinal pathogens, inflammatory bowel disease, irritable bowel syndrome, obesity, celiac disease, non-celiac gluten sensitivity, and food allergies, is associated with a dysfunctional intestinal barrier [61]. Therefore, it can be concluded that because of its anti-oxidant and intestinal barrier crossing functions without any cytotoxic effects, colloidal Pt has the potential to help protect and maintain intestinal health.

Declarations

Author contribution statement

Sinem Tunçer: Conceived and designed the experiments; Performed the experiments; Analyzed and interpreted the data; Wrote the paper.

Melis Çolakoğlu: Performed the experiments; Analyzed and interpreted the data; Wrote the paper.

Sinem Ulusan, Gulay Ertas: Performed the experiments; Analyzed and interpreted the data.

Çimen Karasu: Conceived and designed the experiments.

Sreeparna Banerjee: Conceived and designed the experiments; Performed the experiments; Analyzed and interpreted the data; Contributed reagents, materials, analysis tools or data; Wrote the paper.

Funding statement

Sreeparna Banerjee was supported by Science Academy of Turkey (BAGEP). Sinem Tunçer was supported by a TÜBİTAK 2218 scholarship for postdoctoral fellows. Melis Çolakoğlu was supported by a YÖK 100/2000 PhD scholarship.

Competing interest statement

The authors declare no conflict of interest.

Additional information

Supplementary content related to this article has been published online at https://doi.org/10.1016/j.heliyon.2019.e01336.

References

[1] D. Zhai, B. Liu, Y. Shi, L. Pan, Y. Wang, W. Li, R. Zhang, G. Yu, Highly sensitive glucose sensor based on pt nanoparticle/polyaniline hydrogel heterostructures, ACS Nano (2013).

[2] S. Dasari, P. Bernard Tchounwou, Cisplatin in cancer therapy: molecular mechanisms of action, Eur. J. Pharmacol. (2014).

[3] K. McNamara, S.A.M. Tofail, Nanoparticles in biomedical applications, Adv. Phys. X (2017).

[4] J.P.M. Almeida, E.R. Figueroa, R.A. Drezek, Gold nanoparticle mediated cancer immunotherapy, Nanomed. Nanotechnol. Biol. Med. (2014).

[5] S.N. Sørensen, C. Engelbrekt, H.C.H. Lützhøft, J. Jiménez-Lamana, J.S. Noori, F.A. Alatraktchi, C.G. Delgado, V.I. Slaveykova, A. Baun, A multimethod approach for investigating algal toxicity of platinum nanoparticles, Environ. Sci. Technol. (2016).

[6] P. Konieczny, A.G. Goralczyk, R. Szmyd, L. Skalniak, J. Koziel, F.L. Filon, M. Crosera, A. Cierniak, E.K. Zuba-Surma, J. Borowczyk, E. Laczna, J. Drukala, E. Pyza, D. Semik, O. Woznicka, A. Klein, J. Jura, Effects triggered by platinum nanoparticles on primary keratinocytes, Int. J. Nanomed. (2013).

[7] J. Gopal, N. Hasan, M. Manikandan, H.F. Wu, Bacterial toxicity/compatibility of platinum nanospheres, nanocuboids and nanoflowers, Sci. Rep. (2013).

[8] Y. Saitoh, Y. Yoshimura, K. Nakano, N. Miwa, Platinum nanocolloid-supplemented hydrogen-dissolved water inhibits growth of human tongue carcinoma cells preferentially over normal cells, Exp. Oncol. (2009).

[9] Q. Li, Y. Tanaka, Y. Saitoh, H. Tanaka, N. Miwa, Carcinostatic effects of platinum nanocolloid combined with gamma irradiation on human esophageal squamous cell carcinoma, Life Sci. (2015).

[10] P.V. Asharani, N. Xinyi, M.P. Hande, S. Valiyaveettil, DNA damage and p53-mediated growth arrest in human cells treated with platinum nanoparticles, Nanomedicine (2010).

[11] S. Kato, R. Hokama, H. Okayasu, Y. Saitoh, K. Iwai, N. Miwa, Colloidal platinum in hydrogen-rich water exhibits radical-scavenging activity and improves blood fluidity, J. Nanosci. Nanotechnol. (2012).

[12] S. Raha, B.H. Robinson, Mitochondria, oxygen free radicals, disease and ageing, Trends Biochem. Sci. (2000).

https://doi.org/10.1016/j.heliyon.2019.e01336

[13] M. Nita, A. Grzybowski, The role of the reactive oxygen species and oxidative stress in the pathomechanism of the age-related ocular diseases and other pathologies of the anterior and posterior eye segments in adults, Oxid. Med. Cell. Longev. (2016).

[14] V.I. Lushchak, Free radicals, reactive oxygen species, oxidative stress and its classification, Chem. Biol. Interact. (2014).

[15] P.L. De Sá Junior, D.A.D. Câmara, A.S. Porcacchia, P.M.M. Fonseca, S.D. Jorge, R.P. Araldi, A.K. Ferreira, The roles of ROS in cancer heterogeneity and therapy, Oxid. Med. Cell. Longev. (2017).

[16] E. Birben, U. Murat, C. Sackesen, S. Erzurum, O. Kalayci, Oxidative stress and antioxidant defense, WAO J. (2012).

[17] Y. Liu, H. Wu, M. Li, J.J. Yin, Z. Nie, PH dependent catalytic activities of platinum nanoparticles with respect to the decomposition of hydrogen peroxide and scavenging of superoxide and singlet oxygen, Nanoscale (2014).

[18] A. Watanabe, M. Kajita, J. Kim, A. Kanayama, K. Takahashi, T. Mashino, Y. Miyamoto, In vitro free radical scavenging activity of platinum nanoparticles, Nanotechnology (2009).

[19] T. Aiuchi, S. Nakajo, K. Nakaya, Reducing activity of colloidal platinum nanoparticles for hydrogen peroxide, 2, 2-diphenyl-1-picrylhydrazyl radical and 2, 6-dichlorophenol indophenol, Biol. Pharm. Bull. (2004).

[20] T. Hamasaki, T. Kashiwagi, T. Imada, N. Nakamichi, S. Aramaki, K. Toh, S. Morisawa, H. Shimakoshi, Y. Hisaeda, S. Shirahata, Kinetic analysis of superoxide anion radical-scavenging and hydroxyl radical-scavenging activities of platinum nanoparticles, Langmuir (2008).

[21] M. Fredua-Agyeman, S. Gaisford, Comparative survival of commercial probiotic formulations: tests in biorelevant gastric fluids and real-time measurements using microcalorimetry, Benef. Microbes (2015).

[22] S. Tunçer, S. Banerjee, Determination of autophagy in the Caco-2 spontaneously differentiating model of intestinal epithelial cells, Methods Mol. Biol. (2019).

[23] D. Vllasaliu, F.H. Falcone, S. Stolnik, M. Garnett, Basement membrane influences intestinal epithelial cell growth and presents a barrier to the movement of macromolecules, Exp. Cell Res. (2014).

[24] M. Pfaffl, Quantification strategies in real-time PCR Michael W. Pfaffl, A-Z Quant. PCR (2004).

 https://doi.org/10.1016/j.heliyon.2019.e01336

[25] S.A. Bustin, V. Benes, J.A. Garson, J. Hellemans, J. Huggett, M. Kubista, R. Mueller, T. Nolan, M.W. Pfaffl, G.L. Shipley, J. Vandesompele, C.T. Wittwer, The MIQE guidelines: minimum information for publication of quantitative real-time PCR experiments, Clin. Chem. (2009).

[26] Y. Chen, E. McMillan-Ward, J. Kong, S.J. Israels, S.B. Gibson, Oxidative stress induces autophagic cell death independent of apoptosis in transformed and cancer cells, Cell Death Differ. (2008).

[27] Y. Sambuy, I. De Angelis, G. Ranaldi, M.L. Scarino, A. Stammati, F. Zucco, The Caco-2 cell line as a model of the intestinal barrier: influence of cell and culture-related factors on Caco-2 cell functional characteristics, Cell Biol. Toxicol. (2005).

[28] J. Stetefeld, S.A. McKenna, T.R. Patel, Dynamic light scattering: a practical guide and applications in biomedical sciences, Biophys. Rev. (2016).

[29] P.A. Hassan, S. Rana, G. Verma, Making sense of Brownian motion: colloid characterization by dynamic light scattering, Langmuir (2015).

[30] B. Wessling, Dissipative structure formation in colloidal systems, Adv. Mater. (1993).

[31] F. Kong, R.P. Singh, Disintegration of solid foods in human stomach, J. Food Sci. (2008).

[32] N.P. Farrell, Platinum formulations as anticancer drugs clinical and pre-clinical studies, Curr. Top. Med. Chem. (2011).

[33] C. Burda, X. Chen, R. Narayanan, M.A. El-Sayed, Chemistry and properties of nanocrystals of different shapes, Chem. Rev. (2005).

[34] M.G. Apps, E.H.Y. Choi, N.J. Wheate, The state-of-play and future of platinum drugs, Endocr. Relat. Cancer (2015).

[35] G. Marzun, C. Streich, S. Jendrzej, S. Barcikowski, P. Wagener, Adsorption of colloidal platinum nanoparticles to supports: charge transfer and effects of electrostatic and steric interactions, Langmuir (2014).

[36] R. Serra-Maia, M. Bellier, S. Chastka, K. Tranhuu, A. Subowo, J.D. Rimstidt, P.M. Usov, A.J. Morris, F.M. Michel, Mechanism and kinetics of hydrogen peroxide decomposition on platinum nanocatalysts, ACS Appl. Mater. Interfaces (2018).

[37] V.P. Bindokas, J. Jordán, C.C. Lee, R.J. Miller, Superoxide production in rat hippocampal neurons: selective imaging with hydroethidine, J. Neurosci. 16 (1996) 1324−1336.

https://doi.org/10.1016/j.heliyon.2019.e01336

[38] N. Bryan, H. Ahswin, N. Smart, Y. Bayon, S. Wohlert, J.A. Hunt, Reactive oxygen species (ROS) − a family of fate deciding molecules pivotal in constructive inflammation and wound healing, Eur. Cell. Mater. (2012).

[39] S. Shibuya, Y. Ozawa, K. Watanabe, N. Izuo, T. Toda, K. Yokote, T. Shimizu, Palladium and platinum nanoparticles attenuate aging-like skin atrophy via antioxidant activity in mice, PLoS One (2014).

[40] Y. Yoshihisa, Q.L. Zhao, M.A. Hassan, Z.L. Wei, M. Furuichi, Y. Miyamoto, T. Kondo, T. Shimizu, SOD/catalase mimetic platinum nanoparticles inhibit heat-induced apoptosis in human lymphoma U937 and HH cells, Free Radic. Res. (2011).

[41] S.S.K. Wijeratne, S.L. Cuppett, V. Schlegel, Hydrogen peroxide induced oxidative stress damage and antioxidant enzyme response in Caco-2 human colon cells, J. Agric. Food Chem. (2005).

[42] E.A. Veal, A.M. Day, B.A. Morgan, Hydrogen peroxide sensing and signaling, Mol. Cell. (2007).

[43] C. Lennicke, J. Rahn, R. Lichtenfels, L.A. Wessjohann, B. Seliger, Hydrogen peroxide − production, fate and role in redox signaling of tumor cells, Cell Commun. Signal. (2015).

[44] B. Halliwell, K. Zhao, M. Whiteman, The gastrointestinal tract: a major site of antioxidant action? Free Radic. Res. (2000).

[45] R.K. Rao, R.D. Baker, S.S. Baker, A. Gupta, M. Holycross, Oxidant-induced disruption of intestinal epithelial barrier function: role of protein tyrosine phosphorylation, Am. J. Physiol. (1997).

[46] H.J. Forman, A. Bernardo, K.J.A. Davies, What is the concentration of hydrogen peroxide in blood and plasma? Arch. Biochem. Biophys. (2016).

[47] J.-M. Lü, P.H. Lin, Q. Yao, C. Chen, Chemical and molecular mechanisms of antioxidants: experimental approaches and model systems, J. Cell Mol. Med. (2010).

[48] S.B. Nimse, D. Pal, Free radicals, natural antioxidants, and their reaction mechanisms, RSC Adv. (2015).

[49] K.R. Groschwitz, S.P. Hogan, Intestinal barrier function: molecular regulation and disease pathogenesis, J. Allergy Clin. Immunol. (2009).

[50] E.H. Van Beers, R.H. Al, E.H. Rings, a W. Einerhand, J. Dekker, H. a Büller, Lactase and sucrase-isomaltase gene expression during Caco-2 cell differentiation, Biochem. J. (1995).

https://doi.org/10.1016/j.heliyon.2019.e01336

[51] F.J. Eidelman, A. Fuks, L. DeMarte, M. Taheri, C.P. Stanners, Human carcinoembryonic antigen, an intercellular adhesion molecule, blocks fusion and differentiation of rat myoblasts, J. Cell Biol. (1993).

[52] A.R. Neves, J.F. Queiroz, S.A. Costa Lima, F. Figueiredo, R. Fernandes, S. Reis, Cellular uptake and transcytosis of lipid-based nanoparticles across the intestinal barrier: relevance for oral drug delivery, J. Colloid Interface Sci. (2016).

[53] H. Hillaireau, P. Couvreur, Nanocarriers' entry into the cell: relevance to drug delivery, Cell. Mol. Life Sci. (2009).

[54] S.-H. Bae, J. Yu, M.-R. Go, H.-J. Kim, Y.-G. Hwang, S.-J. Choi, Oral toxicity and intestinal transport mechanism of colloidal gold nanoparticle-treated red ginseng, Nanomaterials (2016).

[55] J. Reinholz, C. Diesler, S. Schöttler, M. Kokkinopoulou, S. Ritz, K. Landfester, V. Mailänder, Protein machineries defining pathways of nanocarrier exocytosis and transcytosis, Acta Biomater. (2018).

[56] M.A. Gatoo, S. Naseem, M.Y. Arfat, A. Mahmood Dar, K. Qasim, S. Zubair, Physicochemical properties of nanomaterials: implication in associated toxic manifestations, BioMed Res. Int. (2014).

[57] A.L. Stepanov, A.N. Golubev, S.I. Nikitin, Y.N. Osin, A review on the fabrication and properties of platinum nanoparticles, Rev. Adv. Mater. Sci. 38 (2) (2014) 160−175.

[58] T.L. Moore, L. Rodriguez-Lorenzo, V. Hirsch, S. Balog, D. Urban, C. Jud, B. Rothen-Rutishauser, M. Lattuada, A. Petri-Fink, Nanoparticle colloidal stability in cell culture media and impact on cellular interactions, Chem. Soc. Rev. (2015).

[59] V. Rashmi, K.R. Sanjay, Green synthesis, characterisation and bioactivity of plant-mediated silver nanoparticles using *Decalepis hamiltonii* root extract, IET Nanobiotechnol. (2017).

[60] S. Mo, X. Shao, Y. Chen, Z. Cheng, Increasing entropy for colloidal stabilization, Sci. Rep. (2016).

[61] J. König, J. Wells, P.D. Cani, C.L. García-Ródenas, T. MacDonald, A. Mercenier, J. Whyte, F. Troost, R.J. Brummer, Human intestinal barrier function in health and disease, Clin. Transl. Gastroenterol. (2016).

https://doi.org/10.1016/j.heliyon.2019.e01336